Chlamydomonas γ-tubulin mutations reveal a critical role of γ-TuRC in maintaining the stability of centriolar microtubules

Yuki Nakazawa[1,2*], Mao Horii[3], Akira Noga[1,3], Yoshikazu Koike[1], Hiroko Kawai-Toyooka[1], Hideo Dohra[4,5], Katsushi Yamaguchi[6], Shuji Shigenobu[6], Ken-ichi Wakabayashi[7], and Masafumi Hirono[1]

[1]Department of Frontier Bioscience, Hosei University, Tokyo, 184-8584, Japan
[2]Science and Technology Group, Okinawa Institute of Science and Technology Graduate University, Okinawa, 904-2245, Japan
[3]Department of Biological Science, Graduate School of Science, University of Tokyo, Tokyo, 113-0033, Japan
[4]Research Institute of Green Science and Technology, Shizuoka University, Shizuoka, 422-8529, Japan.
[5]Shizuoka Instrumental Analysis Center, Shizuoka University, Shizuoka, 426-8668, Japan
[6]Trans-Scale Biology Center, National Institute for Basic Biology, Aichi, 444-8585, Japan
[7]Department of Industrial Life Sciences, Faculty of Life Sciences, Kyoto Sangyo University, Kyoto, 603-8555, Japan

*Corresponding author
E-mail: yuki.nakazawa@oist.jp

Abstract

The centriolar triplet microtubule consists of an A-tubule with 13 protofilaments, and B- and C-tubules, each with 10 protofilaments. Although the formation of the triplets has been shown to require γ-tubulin, its specific role in the formation of each tubule remains elusive. We isolated two novel *Chlamydomonas reinhardtii* mutants, *bld13-1* and *bld13-2*, each expressing γ-tubulin with a single amino-acid substitution (T292I, E89D, respectively). Similar to known centriole-deficient mutants, both mutants exhibited defects in ciliary assembly, nuclear number, and the number and orientation of cytoplasmic microtubules. Genetic analyses of the mutants, along with expression of the mutant γ-tubulins in the wild-type cells, showed that both mutants exert dominant-negative effects over wild-type γ-tubulin. Interestingly, although the centrioles in these mutants retained the typical nine triplet structure, their triplets frequently lacked several protofilaments in specific regions of the A- and C-tubules. The protofilament loss occurs more frequently at the proximal end of the centriole. These structural defects strongly suggest that γ-tubulin is essential for the stability of the A- and C-tubules of centriolar triplets.

Introduction

Triplet microtubules are a specialized type of microtubule found exclusively in centrioles, structures with 9-fold symmetry that serve as the core of the centrosome and the basal bodies of cilia (flagella). Each triplet consists of an A-tubule, composed of 13 protofilaments arranged in a circle, and B- and C-tubules, each composed of 10 protofilaments arranged in an arc. When centrioles function as basal bodies, the outer doublet microtubules of the axoneme extend from the A- and B-tubules (Wang and Stearns, 2017; Osinka et al., 2019; Le Guennec et al., 2021). The unique structure of the centriolar triplet microtubules is highly conserved across eukaryotic organisms, yet its assembly mechanism remains poorly understood (Azimzadeh and Marshall, 2010; Wang and Stearns, 2017; Guichard et al., 2023).

The γ-tubulin ring complex (γ-TuRC) is a major nucleator of microtubules in the cytoplasm (Oakley et al., 2015; Wu and Akhmanova, 2017). It is composed of 14 γ-tubulin molecules arranged in an incomplete ring, along with GCP2~6, MZT1, and other proteins. This structure suggests that it serves as a template for microtubule formation, with each γ-tubulin positioned at the minus end of the protofilament after microtubule assembly (Liu et al., 2021; Thawani and Petry, 2021; Zupa et al., 2021; Sulimenko et al., 2022). In animal cells, numerous γ-TuRCs within the pericentriolar materials (PCM) of

the centrosome nucleate cytoplasmic microtubules, enabling the centrosome to function as the microtubule-organizing center (MTOC) (Oakley et al., 2015; Wu and Akhmanova, 2017).

The γ-TuRC is also essential for centriole formation in many organisms (Ruiz et al., 1999; Shang et al., 2002; Dammermann et al., 2004; Gogendeau et al., 2011; Bahtz et al., 2012; Cota et al., 2017). By analogy to its role in cytoplasmic microtubule nucleation, the γ-TuRC may nucleate the centriolar triplet microtubules. Supporting this hypothesis, cryo-electron microscopy of isolated human centrosomes revealed a conical structure, likely a γ-TuRC, capping the proximal end of the A-tubule in the immature centriole (Guichard et al., 2010). However, the γ-TuRC's nucleation activity for centriolar microtubules has not been directly demonstrated, and its contribution to triplet microtubule assembly and/or maintenance, particularly of the B- and C-tubules, remains unclear.

Besides its prominent localization to the PCM, γ-TuRC is also found various centriolar sites: the proximal region of the triplet microtubule wall, the outer and inner (luminal) surfaces of the microtubule wall, and the distal appendages (Silflow et al., 1999; Schweizer and Lüders, 2021; Kalbfuss and Gönczy, 2023; Laporte et al., 2024). While the specific function of γ-TuRC at each site is unclear, a recent study in human cells showed that the depletion of proteins that localize γ-TuRCs to the inner surfaces of the centriole microtubules destabilizes the centrioles and impairs ciliary assembly (Schweizer et al., 2021). This suggests that the γ-TuRCs within the centriole lumen play a crucial role in maintaining centriole structural integrity.

In this study, we isolated two novel *Chlamydomonas reinhardtii* strains with dominant-negative mutations in the γ-tubulin gene, which exists in a single copy in this organism. These mutants exhibited defects in ciliary assembly, similar to those observed in previously reported centriole-deficient mutants. Intriguingly, their centrioles frequently lacked some of the protofilaments in the A- and C-tubules of triplet microtubules. These phenotypes and the predicted positions of the mutations in the γ-tubulin molecule strongly support the idea that γ-tubulin functions as a γ-TuRC component to stabilize triplet microtubules.

Results

Novel γ-tubulin mutants of *Chlamydomonas*

We isolated two independent *Chlamydomonas* strains that showed defects in ciliary assembly and nuclear segregation, which are phenotypes characteristic of known

centriole-deficient mutants (Figure 1, A and B; Table 1) (Ehler et al., 1995; Dutcher and Trabuco, 1998; Matsuura et al., 2004; Hiraki et al., 2007; Nakazawa et al., 2007). As genetic analyses mapped these mutations to the same locus on Linkage Group VI, we named the mutants *bld13-1* and *bld13-2*, respectively (Figure 1C). Whole genome sequencing of *bld13-1*, and PCR-based sequencing of the *bld13-2* γ-tubulin gene identified point mutations that cause single amino-acid substitutions (*bld13-1*, T292I; *bld13-2*, E89D) in the γ-tubulin gene, a single-copy gene in *Chlamydomonas* (Figure 1D). The original amino acids at these mutation sites are widely conserved among organisms including single-cell organisms and humans (Figure 1D). To infer possible effects of these mutations on the γ-tubulin structure, we compared Alphafold2-predicted models of the *bld13-1* and *bld13-2* γ-tubulins with that of the wild type (Figure S1A) (Jumper et al., 2021). The models suggest no predominant changes in the molecular conformation, except for a slight change in a small region on the molecular surface of *bld13-1* γ-tubulin.

The *bld13-1* and *bld13-2* mutations exhibit dominant-negative effects

The defective phenotypes of the *bld13* mutants were not rescued by expression of a hemagglutinin (HA)-tagged γ-tubulin gene (γ-tub(WT)-HA), suggesting that both mutations might have dominant-negative effects (Figure 2, A and B). To explore this possibility, we produced diploid strains by crossing the wild-type with *bld13-1* or *bld13-2* (WT/*bld13-1*, WT/*bld13-2*), and examined whether they have defects in ciliary assembly. Percentages of cells with no or only one flagellum in the two heterogenic strains are slightly but significantly larger than that of the wild type diploid strain (WT/WT) (Figure 2C). Similar results were obtained when HA-tagged *bld13-1* or *bld13-2* γ-tubulin (WT:: γ-tub(T292I)-HA or WT:: γ-tub(E89D)-HA) was expressed in wild type (Figure 2 A and B). These results suggest that the *bld13-1* and *bld13-2* mutations exert dominant-negative effects over the wild type γ-tubulin gene.

The *bld13* γ-tubulins localize to centrioles

In the interphase *Chlamydomonas* cell, two mature centrioles (basal bodies) and two immature centrioles (probasal bodies) are present at the base of the two cilia, forming an organizing center for four stable rootlet microtubule bundles and non-rootlet cytoplasmic microtubules (Figure 3A; Holmes and Dutcher, 1989). In *bld13-1* or *bld13-2* cells expressing HA-tagged wild-type γ-tubulin (*bld13-1*:: γ-tub(WT)-HA and *bld13-2*:: γ-tub(WT)-HA), HA signals were detected as three or four fluorescent spots at the base of cilia (Figure 3B). Similar localizations of HA signals were observed in wild type cells

expressing HA-tagged *bld13-1* or HA-tagged *bld13-2* γ-tubulin (WT:: γ-tub(T292I)-HA and WT:: γ-tub(E89D)-HA) (Figure 3C). From these observations, we conclude that γ-tubulin-HA is localized to both mature and immature centrioles and that the *bld13-1* and *bld13-2* mutations do not interfere with the localization of HA-tagged wild-type γ-tubulin to the centrioles.

Cytoplasmic microtubule organization is slightly aberrant in *bld13* cells

In mammalian cells, γ-tubulin localizes to the pericentriolar material (PCM) of the centrosome and functions in nucleating and organizing cytoplasmic microtubules (Oakley et al., 2015; Wu and Akhmanova, 2017). In *Chlamydomonas* cells, although obvious PCM has not been observed, functional analogs of PCMs are most likely present, because rootlet and non-rootlet cytoplasmic microtubules extend from the proximity of the centrioles (Holmes and Dutcher, 1989) (Figure 3A). To assess the effects of the *bld13* mutations on the intracellular microtubule-organization, we performed immunofluorescence microscopy using two kinds of tubulin antibodies. Staining with anti-α-tubulin antibody, which recognizes both rootlet and non-rootlet cytoplasmic microtubules, revealed a reduced number of non-rootlet cytoplasmic microtubules and nonuniform inter-microtubule spacing in some *bld13-1* cells. These abnormalities were not evident in *bld13-2* cells (Figure 4A). Staining with anti-acetylated α-tubulin antibody, on the other hand, detected clear differences between the wild type and both of the two mutants (Figure 4B). In wild-type cells, the antibody detects four rootlet microtubules arranged in a cruciform pattern at the base of the cilia. In *bld13-1*, cells were frequently observed that had reduced numbers of rootlet microtubules arranged in abnormal manners. In *bld13-2*, the number of the acetylation-positive microtubules appeared increased, but each microtubule bundle was thinner and shorter than the one in the wild type. Therefore, the *bld13-1* and *bld13-2* γ-tubulins are likely to have some defects in organizing microtubules in *Chlamydomonas* cell bodies.

Centriolar triplet microtubules frequently lack protofilaments in *bld13*

The phenotypes of *bld13* mutants, namely, defective in ciliary assembly, nuclear segregation, and rootlet microtubule organization, are shared by various *Chlamydomonas* mutants having structural defects in the centriole (Ehler et al., 1995; Dutcher and Trabuco, 1998; Matsuura et al., 2004; Hiraki et al., 2007; Nakazawa et al., 2007). Therefore, we examined the centriole structure in *bld13* cells by thin-section electron microscopy. Longitudinal images of *bld13-1* and *bld13-2* centrioles appeared

normal (Figure 5A), although some of those centrioles did not attach axonemes and therefore apparently failed to nucleate ciliary growth. Strikingly, however, obvious defects were observed in cross-sectional images of centrioles in both mutants: some triplet microtubules partially lacked protofilaments (Figure 5B). In most cases, two to seven adjacent protofilaments were lost from particular positions in the A- and C-tubules, but not in the B-tubules. These abnormalities were never observed in wild-type centrioles (Table 2). To evaluate the cross-sectional positions in the *bld13* centrioles where protofilament loss frequently occurs, the cross-sectional images of the A- or C-tubules were divided into 6 or 12 sectors, and the occurrence of missing protofilaments was scored in each sector. The results showed that the protofilament loss frequently occurred in the sectors that contain protofilaments No. A1-A6 of the A-tubule and No. C1- C7 of the C-tubule in both *bld13-1* and *bld13-2* (the numbering is after Linck and Stephens, 2007 and Li et al., 2019) (Figure 5C).

The frequency of the protofilament loss in the A-tubule seemingly varied between the proximal and the distal regions of the centriole. To objectively show this difference, we counted the number of missing protofilaments in four groups of axonemal images that most likely represented distinct positions of the centriole: 1) (transition zone) images with the characteristic star-like structure in the lumen; 2) (distal region) images with distal appendages; 3) (proximal region) images with cartwheels; and 4) (central region), images other than the above three groups (Table 2) (Geimer and Melkonian, 2004; Le Guennec et al., 2021). The results showed that the protofilament loss of the A-tubule was more frequently observed in the proximal region than in the central or distal regions. No protofilament loss was observed in the transition zone. We were unable to examine the regional difference of protofilament loss in the C-tubule, because its image was obscured by electron-dense material near the proximal region and was often missing in the distal region.

Discussion

In this study, we demonstrated that two novel mutations in the γ-tubulin gene in *Chlamydomonas* cause partial loss of protofilaments in centriolar triplet microtubules while having relatively mild effects on the overall centriole structure. The ultrastructural defects observed in the mutant centrioles highlight the crucial role of γ-tubulin in maintaining the stability of triplet microtubules.

Effects of *bld13* mutations on the γ-TuRC assembly

In many eukaryotes, γ-tubulin constitutes two kinds of complexes, one termed the γ-tubulin small complex (γ-TuSCs) and the other termed the γ-tubulin ring complex (γ-TuRC). The γ-TuSC is formed by association between γ-tubulin and two subunits, GCP2 and GCP3; the γ-TuRCs is formed by oligomerization of γ-TuSCs and association with GCP4~6 and MZT1 (Tovey and Conduit, 2018; Böhler et al., 2021). Because *Chlamydomonas* has genes coding for homologs of GCP2~4 and MZT1, γ-tubulin of this organism most likely functions in microtubule nucleation by forming γ-TuRCs.

Both of the two *bld13* mutations in the γ-tubulin gene cause single amino-acid substitutions that do not alter the charge of their side chains (Figure 1). Consistently, Alphafold2 predicts no significant change in the overall molecular structure (Figure S1A). The predicted minor effects of these mutations on the γ-tubulin structure may be correlated with the mild phenotypic abnormalities in the mutants: γ-tubulins are normally localized to centrioles, and cytoplasmic microtubules and ciliary axonemes are formed in most of the mutant cells. On closer look, however, the *bld13* mutations were found to cause apparent defects in microtubule structures in some populations of cells, including abnormal arrangement of rootlet and non-rootlet cytoplasmic microtubules (Figure 4) and partial loss of protofilaments in centriolar microtubules (Figure 5).

We speculate that these defects may result from instability in the association of the γ-tubulin molecules within the γ-TuRC. This is because the mutated amino acid residues in both *bld13* mutants are located on the molecular surface at the region where adjacent γ-tubulin molecules are presumed to interact within the complex (Figure S1B and C; Inclán and Nogales, 2000; Aldaz et al., 2005; Wieczorek et al., 2020). We propose that γ-tubulin molecules are stably held in the complex by inter-subunit interaction at the contact sites, and the *bld13* mutations partially disrupt this interaction. The dominant-negative effects observed with the *bld13* mutations may be due to a weakened inter-γ-tubulin interactions within the γ-TuRCs composed of a mixture of mutant and wild-type γ-tubulin (Figure 2).

It remains unclear how the structural defects in the *bld13* γ-TuRC results in the abnormal organization of the rootlet and non-rootlet microtubules. Since other centriole-deficient mutants, *bld10* and *bld12*, also exhibit abnormal rootlet microtubule arrangement (Matsuura et al., 2004; Nakazawa et al., 2007), it is possible that minor structural defects in the *bld13* centrioles, caused by the protofilament loss, contribute to the cytoplasmic microtubule abnormality. Additionally, *bld13* mutants may have fewer cytoplasmic microtubules than the wild type. This is likely due to the instability of γ-

TuRC in *bld13*, as γ-TuRC is thought to cap and stabilize the minus ends of cytoplasmic microtubules (see below).

γ-tubulin functions in stabilization of centriolar microtubules

The triplet microtubules of *bld13* centrioles frequently lack part of the protofilaments (Figure 5). This type of microtubule defects is unexpected because the lateral interaction between protofilaments is likely essential for the stability of microtubules, and loss of a protofilament would lead to depolymerization of whole microtubules (Gudimchuk and McIntosh, 2021). However, the triplet microtubules in *bld13*, even when lacking protofilaments, do not fully depolymerize. We speculate that this is because they are stabilized by some microtubule-associated structures or proteins, such as the A–C linkers, microtubule inner proteins (MIPs), and the inner-scaffolds of the centriole (Li et al., 2019; Le Guennec et al., 2020). It is interesting to note that the protofilament loss are frequently observed in the region centered on A4 and the region C1-C7, where protofilaments are apparently not associated with those structures or MIPs (Figure 5C).

Protofilament loss in the A-tubule was observed more frequently in the proximal region than in the central or distal region in both *bld13-1* and *bld13-2* centrioles (Table 2), suggesting that the loss was caused by depolymerization from the proximal end of previously formed protofilaments. *In vitro* studies have shown that the γ-TuRC caps the microtubule minus end for a short period and suppresses both polymerization and depolymerization (Wiese and Zheng, 2000; Berman et al., 2023). In centriolar triplet microtubules *in vivo*, their minus ends may be mostly capped by the γ-TuRC, since γ-tubulin has been localized near the proximal ends of the mature centrioles in *Tetrahymena*, *Paramecium*, and mammals (Fuller et al., 1995; Klotz et al., 2003; Joachimiak et al., 2018). Furthermore, cryo-electron tomography of human procentrioles has shown that the A-tubule proximal ends have a conical shape resembling the γ-TuRC-capped microtubule end observed *in vitro* (Guichard et al., 2010). Thus, it is plausible that the γ-TuRC caps the proximal end of the A-tubule to suppress depolymerization, and the *bld13* centrioles are defective in this function due to weakened interaction between γ-tubulin molecules.

Electron microscope observations of the *bld13* centrioles revealed partial loss of protofilaments also in the C-tubules (Figure 5, B and C). The mechanism of the formation and maintenance of B-and C-tubules in centrioles remain unclear, although several proteins including δ-tubulin, ε-tubulin, and CPAP/SAS-4 have been implicated (Hung et al., 2000; Dutcher, 2003; Gogendeau et al., 2011; Zheng et al., 2016; Stathatos et al.,

2021; Vásquez-Limeta et al., 2022; Guichard et al., 2023). Unlike the A-tubule, which has an apparently capped proximal end, the B- and C-tubules have open proximal ends, suggesting distinct mechanisms for their formation. Interestingly, however, a previous study showed that overexpression of a γ-tubulin variant in *Tetrahymena* resulted in B- and C-tubule loss in basal bodies (Joachimiak et al., 2018). This study raises the possibility that γ-tubulin is involved in the assembly or stability of B- and C-tubules also. Our observation of protofilament loss from the centriolar C-tubule in γ-tubulin mutants lends support to this view. We speculate that the γ-TuRC localized to the centriole outer wall may be important for C- and possibly B-tubule stabilization (Schweizer and Lüders, 2021; Kalbfuss and Gönczy, 2023).

In summary, we found that the *bld13* mutations in γ-tubulin lead to a partial loss of protofilaments of centriolar triplet microtubules, while the triplet structure remains stable even when some protofilaments are lost. The loss of protofilaments appears to proceed from the proximal end, potentially due to reduced minus-end capping by the γ-TuRC containing *bld13* γ-tubulin. Our findings have thus highlighted the function of the γ-TuRC and γ-tubulin in stabilizing the minus end of the centriole microtubules, in addition to their established function in initiating tubulin polymerization.

Materials and methods

Chlamydomonas reinhardtii strains

The wild type strains CC124 and CC125, and S1-D2 were obtained from the *Chlamydomonas* Resource Center (University of Minnesota). The mutant *bld13-1* and *bld13-2* were isolated in this study by screening CC125 cells treated with N-methyl-N'-nitro-N-nitrosoguanidine (MNNG) or irradiated with UV, respectively. The diploid strains (WT/*bld13-1*, WT/*bld13-2*, and WT/WT) were produced by crossing two strains with different antibiotic resistance: hygromycin and paromomycin resistance, each conferred by transformation with a plasmid pHyg3 carrying aphVII or pSI103 carrying aphVIII gene by electroporation (Ebersold, 1967; Berthold et al., 2002; Sizova et al., 2001; Yamano et al., 2013). Cells were grown in Tris-acetate-phosphate (TAP) medium with constant illumination (Gorman and Levine, 1965).

Expression of HA-tagged γ-tubulin in *Chlamydomonas*

Genome fragments containing the γ-tubulin gene (Cre06.g299300v5, https://phytozome-next.jgi.doe.gov/) were amplified by PCR with

the primers γ-tub-F (5'-AACTCCCTCACCACCCAGTCA-3') and γ-tub-R (5'-TTTCATTAGGGACCAGGTTAG-3') using genomic DNA of the wild-type, *bld13-1* or *bld13-2*. The amplified fragments were cloned into pCR-Blunt II-TOPO vector (Invitrogen). Into this plasmid, a SpeI fragment containing the aphVII gene excised from pHyg3 was inserted at the SpeI site, and a fragment containing 3×HA-tag sequences digested with NruI/ScaI from p3×HA (Silflow et al., 2001) was inserted at the site adjacent to the stop codon of the γ-tubulin gene. These plasmids were introduced into the wild-type, *bld13-1* or *bld13-2* cells by electroporation using the NEPA21 electroporator (Nepa Gene, Japan) (Yamano et al., 2013). Of the transformants that display resistance to hygromycin, the clones that express the HA-tagged γ-tubulin were screened by Western blotting using anti-HA antibody (3F10, Roche).

Genetic mapping and whole genome sequencing

The mutations *bld13-1* and *bld13-2* were mapped to a region containing the γ-tubulin gene on Chromosome 6 by amplified-fragment-length polymorphism (AFLP)-based analyses of progenies from the mating of these mutants with S1-D2 (Kathir et al., 2003; Nakazawa et al., 2007). Genomic DNA was prepared using the DNeasy Plant Mini kit (QIAGEN) from *bld13-1* cells pretreated with gametolysin to remove the cell wall (Kindle, 1990). A total of 100 ng of genomic DNA was fragmented to an average size of ~350 bp using a Covaris sonicator. Sequence libraries were constructed from the DNA fragments using the TruSeq Nano DNA library prep kit (Illumina), essentially following the manufacturer's instructions. To minimize PCR amplification bias, the number of PCR cycles in the amplification enrichment step was reduced to four. The generated library was evaluated with the Bioanalyzer (Agilent) and then sequenced on a HiSeq 2500 (Illumina) in a 101 x 101 paired-end format.

The sequence reads were aligned onto the *Chlamydomonas* genome sequence version 5.3.1 (Creinhardtii_236.fa.gz) downloaded from the Joint Genome Institute (JGI) (https://phytozome.jgi.doe.gov/pz/portal) using bowtie2 (bowtie-biosourceforge.net/bowtie2/index.shtml). The *bld13-1* mutation was identified by comparing the genome sequence of *bld13-1* with that of CC124 and CC503 focusing on the mapped ~400-kb region on Chromosome 6. The *bld13-2* mutation was identified by PCR amplification and sequencing of the γ-tubulin gene in the *bld13-2* genome.

Western blot analysis

For immunoblotting, whole-cell extracts (10 μg/lane) from *Chlamydomonas* cells were separated by SDS-PAGE and transferred to Immobilon-P membranes (Millipore) as described in Noga et al., 2022. Anti-HA antibody bound to the membrane were detected with goat anti-rat IgG conjugated with horseradish peroxidase (HRP) (Sigma).

Immunofluorescence microscopy

Chlamydomonas cells were fixed and prepared for antibody staining as described previously (Holmes and Dutcher, 1989). Anti-HA antibody (3F10, Roche), anti-α-tubulin antibody (B-5-1-2, Sigma), and anti-acetylated α-tubulin antibody (6-11B-1, Sigma) were used as primary antibodies. Goat anti-mouse IgG conjugated with Alexa Fluor 488, goat anti-mouse IgG conjugated with Alexa Fluor 594, and donkey anti-rat IgG conjugated with Alexa Fluor 594 (Invitrogen) were used as secondary antibodies. Images were obtained with an Axioplan fluorescence microscope (Carl Zeiss MicroImaging) and recorded with a CMOS camera (WRAYCAM-NOA2000, WRAYMER).

Electron microscopy

Logarithmically growing cells were prefixed with 2% glutaraldehyde in 0.1 M S-collidine buffer for 1–2 hr at 0ºC and postfixed with 1% OsO4 in the same buffer for 1-2 hr (Wright et al., 1983). The specimens were then dehydrated and embedded in EPON 812. Thin sections (50–70 nm) were stained with aqueous uranyl acetate and Reynold's lead citrate and observed with JEM-1400plus at 80 kV or JEM-1230R at 100 kV (JEOL).

Analysis of protofilament loss in centriolar triplet microtubules

To evaluate triplet microtubule integrity, we collected electron microscope images of triplet microtubules in the distal, central and proximal regions of the A tubule, and the central region of the C-tubule of *bld13-1* and *bld13-2* centrioles (Table 2) based on the clarity of the protofilaments. Potential intrinsic variation among the nine triplets within each centriole was not considered during image selection. To evaluate protofilament loss, each tubule image was divided into sectors (12 for the A-tubule and 6 for the C-tubule), and the number of missing protofilaments in each sector was scored (Figure 5C). Missing protofilaments were scored in sectors rather than in numbered protofilaments because the images often lacked sufficient resolution to identify specific protofilament numbers. The B-tubule did not show any protofilament loss.

Acknowledgements

We thank Dr. Ritsu Kamiya (Chuo University) for critically reading the manuscript, Dr. Takako Kato-Minoura (Chuo Univ.) and OIST Imaging Section for use of electron microscopes, OIST Memory Research Unit, OIST Evolution, Cell biology, Symbiosis Unit, OIST Membrenology Unit, Dr. Midori Ohta (OIST), Dr. Petra Svetlikova (OIST), Dr. Yohsuke Moriyama (OIST) and Dr. Akane Furuta (NICT) for helpful advice and fruitful discussions. This work was supported by JSPS KAKENHI (16J40154 to YN, 23K23905 to KW, and 21K06257 and 24K02055 to MH). This work was also supported in part by NIBB Collaborative Research Program (14733) to KW.

References

Aldaz H, Rice LM, Stearns T, Agard DA (2005). Insights into microtubule nucleation from the crystal structure of human gamma-tubulin. *Nature* 435, 523-7.

Azimzadeh J, Marshall WF (2010). Building the centriole. *Curr Biol* 20, R816-25.

Bahtz R, Seidler J, Arnold M, Haselmann-Weiss U, Antony C, Lehmann WD, Hoffmann I (2012). GCP6 is a substrate of Plk4 and required for centriole duplication. *J Cell Sci* 125, 486-496.

Berman AY, Wieczorek M, Aher A, Olinares PDB, Chait BT, Kapoor TM (2023). A nucleotide binding-independent role for γ-tubulin in microtubule capping and cell division. *J Cell Biol* 222, e202204102.

Berthold P, Schmitt R, Mages W (2002). An engineered Streptomyces hygroscopicus aph 7" gene mediates dominant resistance against hygromycin B in *Chlamydomonas reinhardtii*. *Protist* 153, 401-412.

Böhler A, Vermeulen BJA, Würtz M, Zupa E, Pfeffer S, Schiebel E (2021). The gamma-tubulin ring complex: Deciphering the molecular organization and assembly mechanism of a major vertebrate microtubule nucleator. *Bioessays* 43, e2100114.

Cota RR, Teixidó-Travesa N, Ezquerra A, Eibes S, Lacasa C, Roig J, Lüders J (2017). MZT1 regulates microtubule nucleation by linking γTuRC assembly to adapter-mediated targeting and activation. *J Cell Sci* 130, 406-419.

Dammermann A, Müller-Reichert T, Pelletier L, Habermann B, Desai A, Oegema K (2004). Centriole assembly requires both centriolar and pericentriolar material proteins. *Dev Cell* 7, 815-829.

Dutcher SK, Trabuco EC (1998). The UNI3 gene is required for assembly of basal bodies of *Chlamydomonas* and encodes delta-tubulin, a new member of the tubulin superfamily. *Mol Biol Cell* 9, 1293-1308.

Dutcher SK (2003). Long-lost relatives reappear: identification of new members of the

tubulin superfamily. *Curr Opin Microbiol* 6, 634-640.

Ebersold WT (1967). *Chlamydomonas reinhardi*: heterozygous diploid strains. Science 157, 447-449.

Ehler LL, Holmes JA, Dutcher SK (1995). Loss of spatial control of the mitotic spindle apparatus in a *Chlamydomonas reinhardtii* mutant strain lacking basal bodies. *Genetics* 141, 945-960.

Fuller SD, Gowen BE, Reinsch S, Sawyer A, Buendia B, Wepf R, Karsenti E (1995). The core of the mammalian centriole contains gamma-tubulin. *Curr Biol* 5, 1384-1393.

Geimer S, Melkonian M (2004). The ultrastructure of the *Chlamydomonas reinhardtii* basal apparatus: identification of an early marker of radial asymmetry inherent in the basal body. *J Cell Sci* 117, 2663-2674.

Gogendeau D, Hurbain I, Raposo G, Cohen J, Koll F, Basto R (2011). Sas-4 proteins are required during basal body duplication in Paramecium. *Mol Biol Cell* 22, 1035-1044.

Gorman DS, Levine RP (1965) . Cytochrome f and plastocyanin: their sequence in the photosynthetic electron transport chain of *Chlamydomonas reinhardi*. *Proc Natl Acad Sci U S A* 54, 1665-1669.

Gudimchuk NB, McIntosh JR (2021). Regulation of microtubule dynamics, mechanics and function through the growing tip. *Nat Rev Mol Cell Biol* 22, 777-795.

Guichard P, Chrétien D, Marco S, Tassin AM (2010). Procentriole assembly revealed by cryo-electron tomography. *EMBO J* 29, 1565-1572.

Guichard P, Laporte MH, Hamel V (2023). The centriolar tubulin code. *Semin Cell Dev Biol* 137, 16-25.

Hiraki M, Nakazawa Y, Kamiya R, Hirono M (2007). Bld10p constitutes the cartwheel-spoke tip and stabilizes the 9-fold symmetry of the centriole. *Curr Biol* 17, 1778-1783.

Holmes JA, Dutcher SK (1989). Cellular asymmetry in *Chlamydomonas reinhardtii. J Cell Sci* 94, 273-285.

Hung LY, Tang CJ, Tang TK (2000). Protein 4.1 R-135 interacts with a novel centrosomal protein (CPAP) which is associated with the gamma-tubulin complex. *Mol Cell Biol* 20, 7813-7825.

Inclán YF, Nogales E (2001). Structural models for the self-assembly and microtubule interactions of gamma-, delta- and epsilon-tubulin. *J Cell Sci* 114, 413-422.

Joachimiak E, Jerka-Dziadosz M, Krzemień-Ojak Ł, Wacławek E, Jedynak K, Urbanska P, Brutkowski W, Sas-Nowosielska H, Fabczak H, Gaertig J, Wloga D (2018). Multiple phosphorylation sites on γ-tubulin are essential and contribute to the biogenesis of basal bodies in Tetrahymena. *J Cell Physiol*, 1–18.

Jumper J, Evans R, Pritzel A, Green T, Figurnov M, Ronneberger O, Tunyasuvunakool K, Bates R, Žídek A, Potapenko A, Bridgland A, Meyer C, Kohl SAA, Ballard AJ, Cowie A, Romera-Paredes B, Nikolov S, Jain R, Adler J, Back T, Petersen S, Reiman D, Clancy E, Zielinski M, Steinegger M, Pacholska M, Berghammer T, Bodenstein S, Silver D, Vinyals O, Senior AW, Kavukcuoglu K, Kohli P, Hassabis D (2021). Highly accurate protein structure prediction with AlphaFold. *Nature* 596, 583-589.

Kalbfuss N, Gönczy P (2023). Towards understanding centriole elimination. *Open Biol* 13, 230222.

Kathir P, LaVoie M, Brazelton WJ, Haas NA, Lefebvre PA, Silflow CD (2003). Molecular map of the *Chlamydomonas reinhardtii* nuclear genome. *Eukaryot Cell* 2, 362-379.

Kindle KL (1990). High-frequency nuclear transformation of *Chlamydomonas reinhardtii. Proc Natl Acad Sci U S A* 87, 1228-1232.

Klotz C, Ruiz F, Garreau de Loubresse N, Wright M, Dupuis-Williams P, Beisson J (2003). Gamma-tubulin and MTOCs in Paramecium. *Protist* 154, 193-209.

Laporte MH, Gambarotto D, Bertiaux É, Bournonville L, Louvel V, Nunes JM, Borgers S,

Hamel V, Guichard P (2024). Time-series reconstruction of the molecular architecture of human centriole assembly. *Cell* 187, 2158-2174.e19.

Le Guennec M, Klena N, Gambarotto D, Laporte MH, Tassin AM, van den Hoek H, Erdmann PS, Schaffer M, Kovacik L, Borgers S, Goldie KN, Stahlberg H, Bornens M, Azimzadeh J, Engel BD, Hamel V, Guichard P (2020). A helical inner scaffold provides a structural basis for centriole cohesion. *Sci Adv* 6, eaaz4137.

Le Guennec M, Klena N, Aeschlimann G, Hamel V, Guichard P (2021). Overview of the centriole architecture. *Curr Opin Struct Biol* 66, 58-65.

Li JB, Gerdes JM, Haycraft CJ, Fan Y, Teslovich TM, May-Simera H, Li H, Blacque OE, Li L, Leitch CC, Lewis RA, Green JS, Parfrey PS, Leroux MR, Davidson WS, Beales PL, Guay-Woodford LM, Yoder BK, Stormo GD, Katsanis N, Dutcher SK (2004). Comparative genomics identifies a flagellar and basal body proteome that includes the BBS5 human disease gene. *Cell* 117, 541-52.

Li S, Fernandez JJ, Marshall WF, Agard DA (2019). Electron cryo-tomography provides insight into procentriole architecture and assembly mechanism. *Elife* 8, e43434.

Linck RW, Stephens RE (2007). Functional protofilament numbering of ciliary, flagellar, and centriolar microtubules. *Cell Motil Cytoskeleton* 64, 489-495.

Liu P, Würtz M, Zupa E, Pfeffer S, Schiebel E (2021). Microtubule nucleation: The waltz between γ-tubulin ring complex and associated proteins. *Curr Opin Cell Biol* 68, 124-131.

Matsuura K, Lefebvre PA, Kamiya R, Hirono M (2004). Bld10p, a novel protein essential for basal body assembly in *Chlamydomonas*: localization to the cartwheel, the first ninefold symmetrical structure appearing during assembly. *J Cell Biol* 165, 663-671.

Nakazawa Y, Hiraki M, Kamiya R, Hirono M (2007). SAS-6 is a cartwheel protein that establishes the 9-fold symmetry of the centriole. *Curr Biol* 17, 2169-2174.

Noga A, Horii M, Goto Y, Toyooka K, Ishikawa T, Hirono M (2022). Bld10p/Cep135 determines the number of triplets in the centriole independently of the cartwheel. *EMBO*

J 41, e104582.

Oakley BR, Paolillo V, Zheng Y (2015). γ-Tubulin complexes in microtubule nucleation and beyond. *Mol Biol Cell* 26, 2957-2962.

Osinka A, Poprzeczko M, Zielinska MM, Fabczak H, Joachimiak E, Wloga D (2019). Ciliary Proteins: Filling the Gaps. Recent Advances in Deciphering the Protein Composition of Motile Ciliary Complexes. *Cells* 8, 730.

Pazour GJ, Agrin N, Leszyk J, Witman GB (2005). Proteomic analysis of a eukaryotic cilium. *J Cell Biol* 170, 103-13.

Ruiz F, Beisson J, Rossier J, Dupuis-Williams P (1999) . Basal body duplication in Paramecium requires gamma-tubulin. *Curr Biol* 9, 43-46.

Schweizer N, Haren L, Dutto I, Viais R, Lacasa C, Merdes A, Lüders J (2021). Sub-centrosomal mapping identifies augmin-γTuRC as part of a centriole-stabilizing scaffold. *Nat Commun* 12, 6042.

Schweizer N, Lüders J (2021). From tip to toe - dressing centrioles in γTuRC. *J Cell Sci* 134, jcs258397.

Shang Y, Li B, Gorovsky MA (2002). Tetrahymena thermophila contains a conventional gamma-tubulin that is differentially required for the maintenance of different microtubule-organizing centers. *J Cell Biol* 158, 1195-1206.

Sievers F, Higgins DG (2014). Clustal omega. *Curr Protoc Bioinformatics* 48, 3.13.1-3.13.16.

Silflow CD, Liu B, LaVoie M, Richardson EA, Palevitz BA (1999). Gamma-tubulin in *Chlamydomonas*: characterization of the gene and localization of the gene product in cells. *Cell Motil Cytoskeleton* 42, 285-97.

Silflow CD, LaVoie M, Tam LW, Tousey S, Sanders M, Wu W, Borodovsky M, Lefebvre PA (2001). The Vfl1 Protein in *Chlamydomonas* localizes in a rotationally asymmetric pattern at the distal ends of the basal bodies. *J Cell Biol* 153, 63-74.

Sizova I, Fuhrmann M, Hegemann P (2001). A Streptomyces rimosus aphVIII gene coding for a new type phosphotransferase provides stable antibiotic resistance to *Chlamydomonas reinhardtii*. *Gene* 277, 221-229.

Stathatos GG, Dunleavy JEM, Zenker J, O'Bryan MK (2021). Delta and epsilon tubulin in mammalian development. *Trends Cell Biol* 31, 774-787.

Sulimenko V, Dráberová E, Dráber P (2022). γ-Tubulin in microtubule nucleation and beyond. *Front Cell Dev Biol* 10, 880761.

Thawani A, Petry S (2021). Molecular insight into how γ-TuRC makes microtubules. *J Cell Sci* 134, jcs245464.

Tovey CA, Conduit PT (2018). Microtubule nucleation by γ-tubulin complexes and beyond. *Essays Biochem* 62, 765-780.

Vásquez-Limeta A, Lukasik K, Kong D, Sullenberger C, Luvsanjav D, Sahabandu N, Chari R, Loncarek J (2022). CPAP insufficiency leads to incomplete centrioles that duplicate but fragment. *J Cell Biol* 221, e202108018.

Wang JT, Stearns T (2017). The ABCs of Centriole Architecture: The Form and Function of Triplet Microtubules. *Cold Spring Harb Symp Quant Biol* 82, 145-155.

Wieczorek M, Urnavicius L, Ti SC, Molloy KR, Chait BT, Kapoor TM (2020). Asymmetric Molecular Architecture of the Human γ-Tubulin Ring Complex. *Cell* 180, 165-175.e16.

Wiese C, Zheng Y (2000). A new function for the gamma-tubulin ring complex as a microtubule minus-end cap. *Nat Cell Biol* 2, 358-364.

Wright RL, Salisbury J, Jarvik JW (1985). A nucleus-basal body connector in *Chlamydomonas reinhardtii* that may function in basal body localization or segregation. *J*

Cell Biol 101, 1903-1912.

Wu J, Akhmanova A (2017). Microtubule-Organizing Centers. *Annu Rev Cell Dev Biol* 33, 51-75.

Yamano T, Iguchi H, Fukuzawa H (2013). Rapid transformation of *Chlamydomonas reinhardtii* without cell-wall removal. *J Biosci Bioeng* 115, 691-694.

Zheng X, Ramani A, Soni K, Gottardo M, Zheng S, Ming Gooi L, Li W, Feng S, Mariappan A, Wason A, Widlund P, Pozniakovsky A, Poser I, Deng H, Ou G, Riparbelli M, Giuliano C, Hyman AA, Sattler M, Gopalakrishnan J, Li H (2016). Molecular basis for CPAP-tubulin interaction in controlling centriolar and ciliary length. *Nat Commun* 7, 11874.

Zupa E, Liu P, Würtz M, Schiebel E, Pfeffer S (2021). The structure of the γ-TuRC: a 25-years-old molecular puzzle. *Curr Opin Struct Biol* 66, 15-21.

Table 1. Abnormal nuclear segregation in the *bld13* mutants

Strain	Number of nuclei/cell (n>2200)			
	0	1	2 or 3	
wild type	0.61	99.30	0.09	
bld12-1	3.70	90.20	6.11	
bld13-1	1.24	95.34	3.43	
bld13-2	0.64	98.39	0.97	(%)

Table 2. Frequencies of triplet images with partial protofilament loss (%)

Strain		Regions in longitudinal axis of the centriole				
		Transition zone	Distal	Central	Proximal	
		n>60	n>50	n>50	n>30	
Wild type	A-tubule	ND	0.0	0.0	0.0	
	C-tubule	ND	ND	0.0	ND	
bld13-1	A-tubule	0.0	4.0	23.3	37.1	
	C-tubule	ND	ND	12.3	ND	
bld13-2	A-tubule	0.0	0.0	9.6	16.7	
	C-tubule	ND	ND	23.9	ND	(%)

Figures

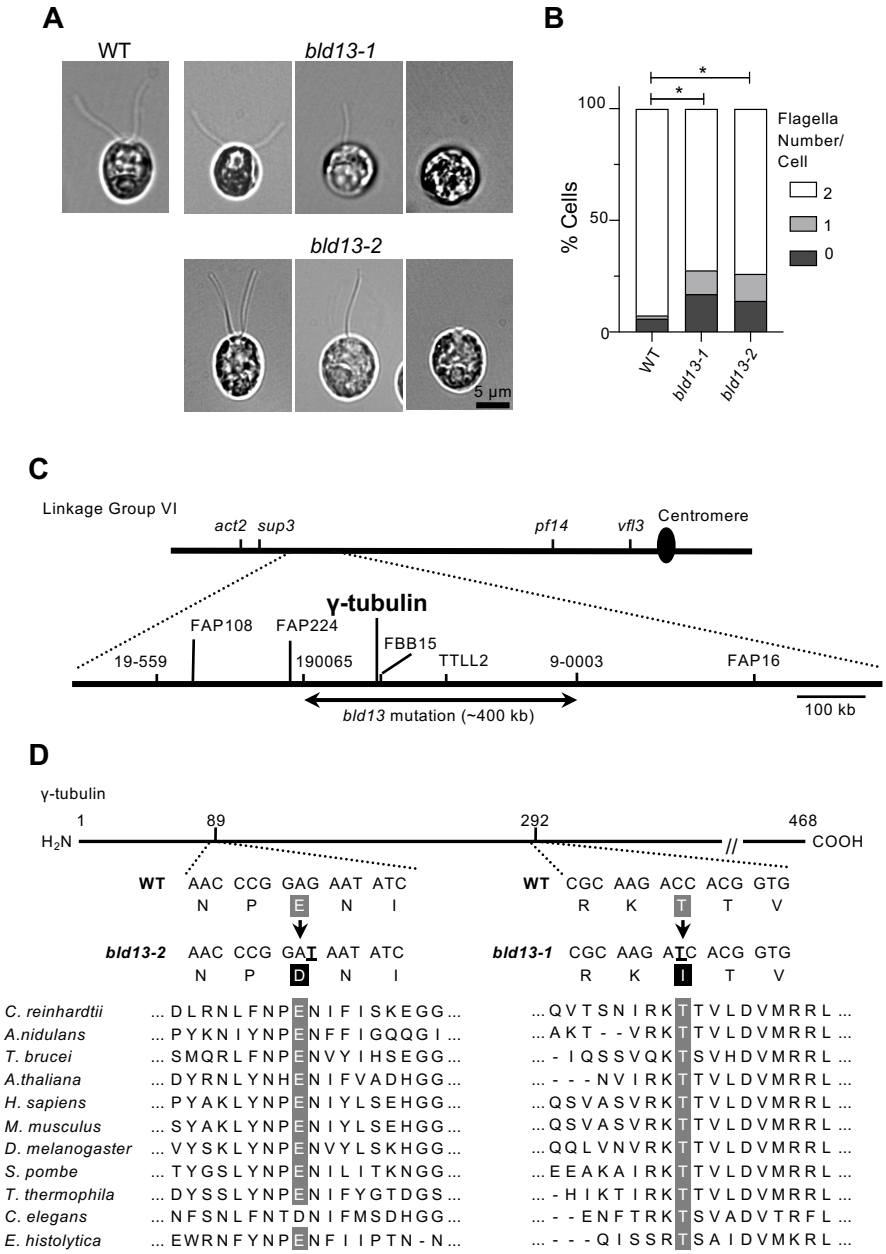

Figure 1.

Novel *Chlamydomonas* mutants *bld13-1* and *bld13-2*. (A) Phase contrast images of wild-type, *bld13-1* and *bld13-2* cells. Both *bld13* mutants contain cells with no or one flagellum in addition to cells with two cilia. (B) Percentages of cells with zero, one, or two cilia in wild type (WT), *bld13-1*, and *bld13-2*. (χ^2 test, *P<0.05, n>350). (C) A genetic map showing a part of Linkage Group VI. The *bld13-1* and *bld13-2* mutations were mapped to an ~400-kb region in this linkage group by AFLP-based analyses. The upper line shows the corresponding locus on the genetic map constructed by Kathir et al. (Kathir et al., 2003). The lower line shows positions of genes around this region (JGI Phytozome v 13, *Chlamydomonas* database v 5.6 https://phytozome-next.jgi.doe.gov/).

Numbers 19-559, 190065, and 9-0003 represent primer sets used for PCR. FAP16, FAP108, and FAP224 are genes of flagellar associated proteins (Pazour et al., 2005), FBB15 is a flagella/basal body protein gene (Li et al., 2004), and TTLL2 is a putative tubulin tyrosine ligase gene (Cre06.g300250, JGI Phytozome v 13, *Chlamydomonas* database v 5.6, https://phytozome-next.jgi.doe.gov/). (D) The positions of the *bld13-1* and *bld13- 2* mutations in the γ-tubulin amino acid sequence of *Chlamydomonas* and corresponding sequences in other organisms. GenBank accession numbers are as follows: *C. reinhardtii*, AAA82610.1; *A. nidulans*, CAA33507.1; *T. brucei*, XP_843687.1; *A. thaliana*, NP_191724.1; *H. sapiens*, NP_001061.2; *M. musculus*, NP_598785.1; *D. melanogaster*, NP_476804.1; *S. pombe*, NP_596147.1; *T. thermophila*, AAB65830.1; *C. elegans*, NP_499131.1; *E. histolytica*, AAC08441.1.

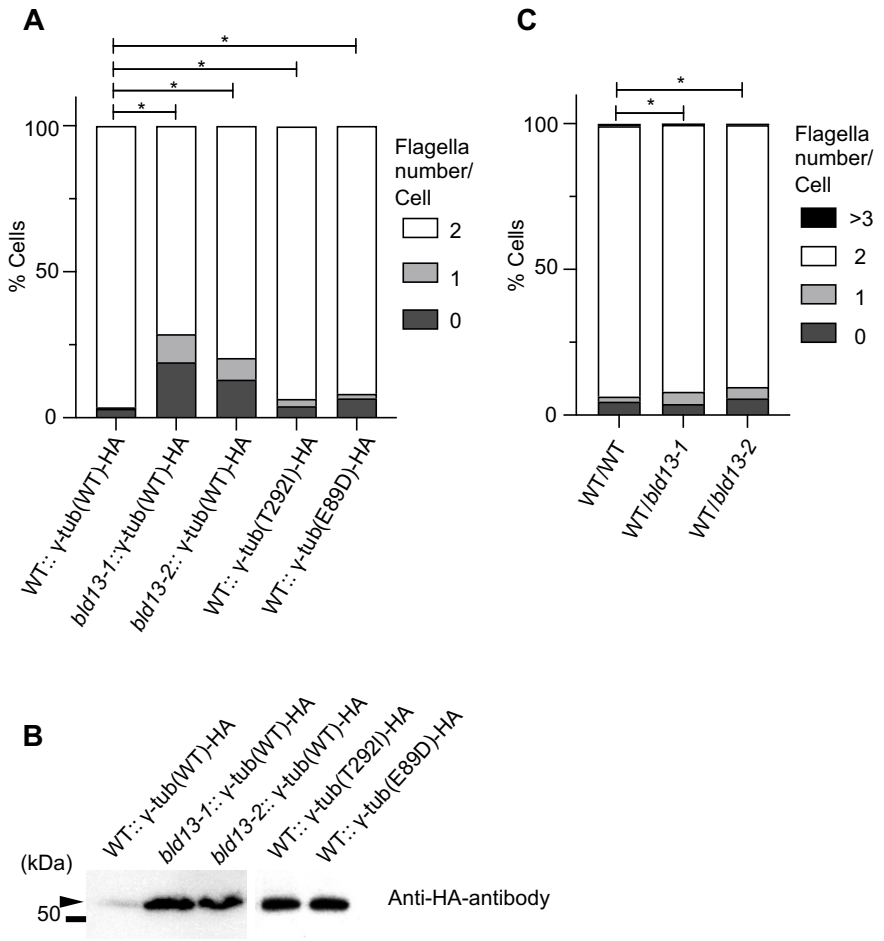

Figure 2.

Dominant negative effects of the *bld13* mutations on ciliary assembly. (A) Percentages of cells with zero, one, or two cilia in a wild type strain expressing an HA-tagged γ-tubulin (WT::γ-tub (WT)-HA), a *bld13-1* strain expressing the HA-tagged γ-tubulin (*bld13-1*::γ-tub (WT)-HA), a *bld13-2* strain expressing the HA-tagged γ-tubulin (*bld13-2*::γ-tub (WT)-HA), a wild type strain expressing the *bld13-1* γ-tubulin (WT::γ-tub (T292I)-HA), and a wild type strain expressing the *bld13-2* γ-tubulin (WT::γ-tub (E89D)-HA). (χ^2 test, *P<0.05, n>1000). (B) Western blot analyses of whole cell lysates (10 μg/lane) of WT::γ-tub (WT)-HA, *bld13-1*::γ-tub (WT)-HA, *bld13-2*::γ-tub (WT)-HA, WT::γ-tub (T292I)-HA, and WT::γ-tub (E89D)-HA cells. Anti-HA antibody detected γ-tubulin (WT)-HA (55 kDa; arrowhead). Despite repeated attempts, HA-tagged wild-type (WT) γ-tubulin was expressed in much lower level in recombinants of WT cells compared with recombinant *bld13-1* or *bld13-2* cells. The reason is not understood. (C) Percentages of cells with zero, one, or two cilia in a diploid strain of the wild type (WT/WT), a strain heterozygous for *bld13-1* (WT/*bld13-1*), and for *bld13-2* (WT/*bld13-2*).

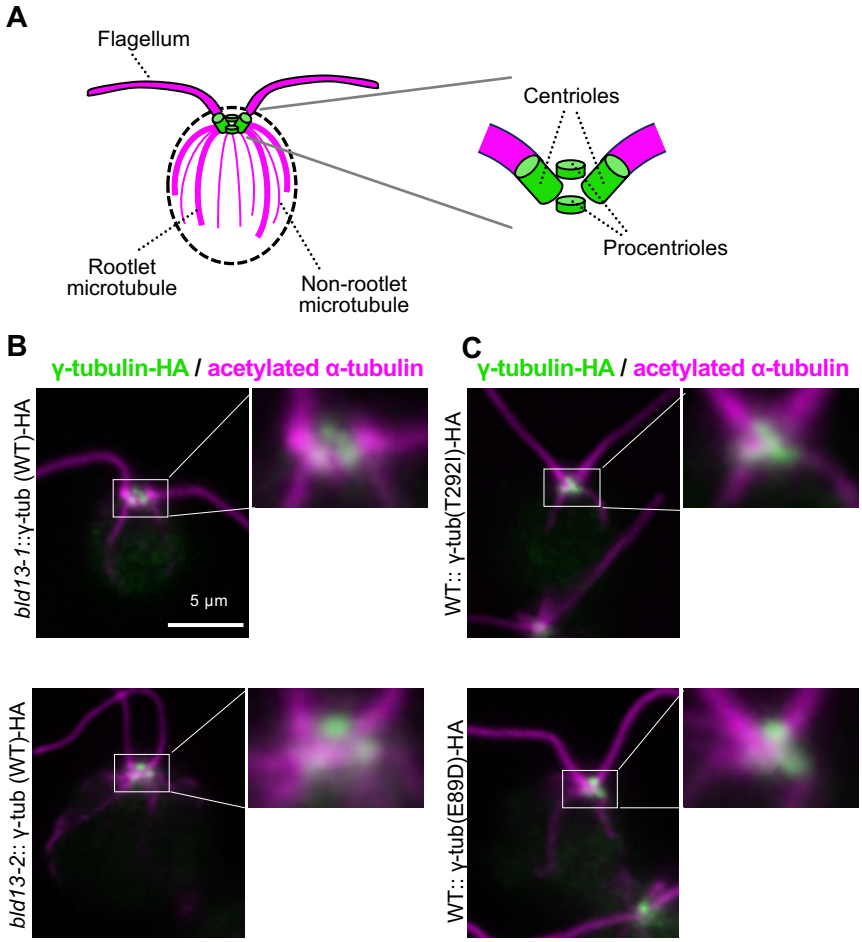

Figure 3.

Effects of the *bld13* mutations on the localization of γ-tubulin. (A) Schematic diagram of microtubule organization in the *Chlamydomonas* cell. (B) Immunofluorescence images of *bld13-1*::γ-tub (WT)-HA and *bld13-2*::γ-tub (WT)-HA cells stained with anti-acetylated-α-tubulin (magenta) and anti-HA (green) antibodies. Right panels are magnified views of the boxed regions in the left panels. C) Immunofluorescence images of WT::γ-tub (T292I)-HA and WT::γ-tub (E89D)-HA cells double-stained with anti-acetylated-α-tubulin (magenta) and anti-HA (green) antibodies. Right panels are magnified views of the boxed regions in the left panels.

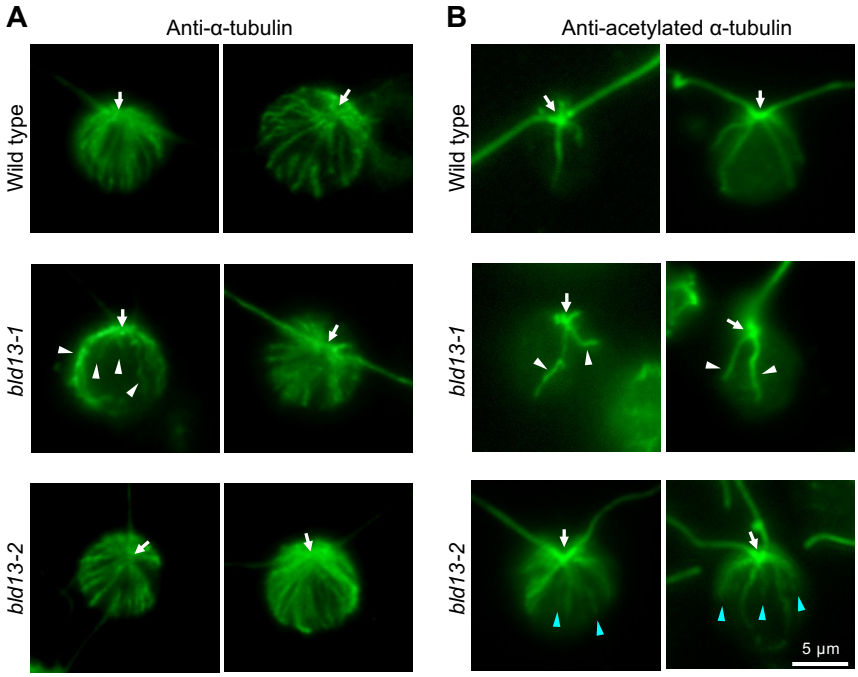

Figure 4.

Effects of *bld13* mutations on microtubule organization in *Chlamydomonas* cells. (A) Immunofluorescence images of wild-type, *bld13-1* and *bld13-2* cells stained with anti-α-tubulin antibody, which recognizes rootlet, non-rootlet, centriolar, and axonemal microtubules. Arrows indicate the position of the centrioles (basal bodies). Arrowheads indicate cytoplasmic microtubules that are abnormal in number, length, and arrangement. Such abnormality was found in 10-20% of *bld13-1* cells but not in *bld13-2*. (B) Immunofluorescence images of wild-type, *bld13-1*, and *bld13-2* cells stained with anti-acetylated α-tubulin antibody, which recognizes rootlet, axonemal, and centriolar microtubules, but not non-rootlet cytoplasmic microtubules (Holmes and Dutcher, 1989). Arrows indicate the position of the centrioles. Arrowheads indicate rootlet microtubules in *bld13-1* cells that are abnormal in number and arrangement. Cyan arrowheads indicate an increased number of short acetylated microtubules in *bld13-2* cells.

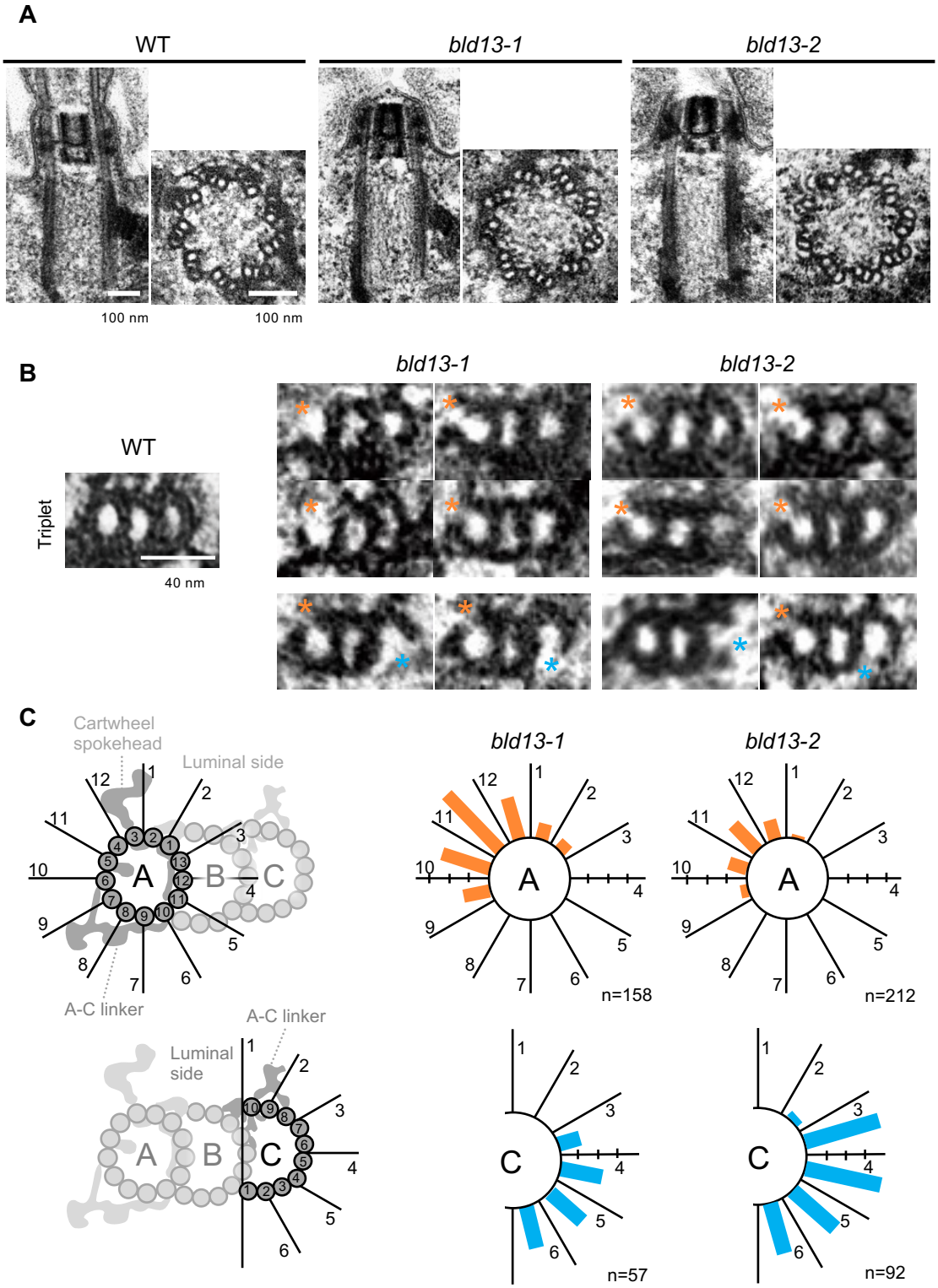

Figure 5.

Partial loss of protofilaments in *bld13* centriolar triplet microtubules. (A) Electron microscopic images of longitudinal and cross sections of centrioles in WT, *bld13-1*, and *bld13-2* cells. (B) Magnified views of cross-sections of the triplet microtubules in WT, *bld13-1*, and *bld13-2* centrioles. Asterisks indicate the positions of protofilament loss. (C) Distributions of the protofilament loss in A- and C-tubules of *bld13-1* and *bld13-*

2 triplet microtubules. A cross-sectional image of the A- or C-tubule was divided into 12 or 6 sectors as shown in schematic diagrams (left, see Materials and Methods). MIPs (in the lumen of the A-tubule), A-C linker, and cartwheel spokehead, are drawn in grey (Li et al., 2019). The length of each bar in the polar histograms (right) represents the relative frequency of protofilament loss at the corresponding sector. The X-axis of each graph is marked in 5% increments. All distributions of the protofilament loss are significantly non-uniform (Hodges-Ajne test): *bld13-1* A-tubule ($P < 0.0001$, median: sector 11), *bld13-2* A-tubule ($P < 0.0001$, median: sector 11), *bld13-1* C-tubule ($P < 0.0001$, median: sector 4), *bld13-2* C-tubule ($P < 0.0001$, median: sector 4).